

PROBLEMS FOR MODIFIED NEWTONIAN DYNAMICS IN CLUSTERS AND THE Ly α FOREST?

ANTHONY AGUIRRE, JOOP SCHAYE, AND ELIOT QUATAERT¹

School of Natural Sciences, Institute for Advanced Study, Einstein Drive, Princeton, NJ 08540; aguirre@ias.edu, schaye@ias.edu, eliot@ias.edu

Received 2001 May 10; accepted 2001 July 17

ABSTRACT

The observed dynamics of gas and stars on galactic and larger scales cannot be accounted for by self-gravity, indicating that there are large quantities of unseen matter or that gravity is non-Newtonian in these regimes. Milgrom’s modified Newtonian dynamics (MOND) postulates that Newton’s laws are modified at very low acceleration, and can account for the rotation curves of galaxies and some other astrophysical observations, without dark matter. Here we apply MOND to two independent physical systems: Ly α absorbers and galaxy clusters. While physically distinct, both are simple hydrodynamical systems with characteristic accelerations in the MOND regime. We find that, because MOND violates the strong equivalence principle, the properties of Ly α absorbers depend strongly on the (unknown) background acceleration field in which they are embedded. If this field is small compared to their internal accelerations, then the absorbers are more dense and about 10 times smaller than in Newtonian gravity with dark matter, in conflict with sizes inferred from quasar pair studies. If, however, the background field is rather large, then the absorbers take on properties similar to those predicted in the cold dark matter picture. In clusters MOND appears to explain the observed (baryonic) mass-temperature relation. However, given observed gas density and enclosed mass profiles and the assumption of hydrostatic equilibrium, MOND predicts radial temperature profiles that disagree badly with observations. We show this explicitly for the Virgo, Abell 2199, and Coma Clusters, but the results are general and seem very difficult to avoid. If this discrepancy is to be resolved by positing additional (presumably baryonic) dark matter, then this dark matter must have ~ 1 – 3 times the cluster gas mass within 1 Mpc and about 10 times the gas mass within 200 kpc. This result strongly disfavors MOND as an alternative to dark matter.

Subject headings: cosmology: theory — dark matter — galaxies: clusters: general — gravitation — hydrodynamics — intergalactic medium

1. INTRODUCTION

The currently most widely accepted “standard model” of cosmology holds that the vast majority of the mass density of the universe is hidden in dark forms. The rotation curves of galaxies and the dynamics of galaxy clusters cannot be accounted for by the gravitation of visible stars and gas, while constraints from primordial nucleosynthesis studies imply that the additional “dark matter” postulated to remedy this discrepancy must be nonbaryonic. On a cosmological level, collisionless (or very weakly collisional) dark matter is required if primordial density perturbations of amplitude $\Delta\rho/\rho \sim 10^{-5}$ are to grow quickly enough to form galaxies by the present epoch. Finally, recent determinations of the high-redshift Type Ia supernova Hubble diagram, in tandem with microwave background data implying a flat cosmic geometry, and a large collection of data indicating that clustering matter contributes only $\sim 30\%$ of the critical density imply that the universe also contains “dark energy” of a yet more exotic form that causes acceleration in the cosmic expansion (see, e.g., Peebles 1999 and Turner 1999 for recent reviews).

Discomfort with this repeated postulation of invisible matter with increasingly unusual properties has led some, quite reasonably, to ask whether the observed phenomena could be accounted for not by the presence of unseen matter but by a departure from Newtonian/Einsteinian dynamics in the regime where dark matter is hypothesized to be important. Perhaps the most successful of such proposals is

the modified Newtonian dynamics (MOND) proposed by Milgrom (1983a, 1983b, 1983c), in which Newtonian dynamics breaks down below an acceleration threshold of $a_0 \sim 10^{-8} \text{ cm s}^{-2}$. Successes of this theory are that it accounts for the rotation curves of galaxies of various luminosities (Sanders & Verheijen 1998) and surface brightnesses (de Blok & McGaugh 1998; McGaugh & de Blok 1998), accounts for the Tully-Fisher and Faber-Jackson relations (van den Bosch & Dalcanton 2000; Sanders 1996, 2000), and—arguably—roughly accounts for the amount of dark matter inferred in clusters (Sanders 1999).

Despite some attempts, MOND has not been generalized into a satisfactory relativistic theory that can yield unambiguous cosmological predictions. However, in light of MOND’s general success when applied to galaxies and the current lack of any decisive empirical argument against it, it is worth investigating whether MOND works in detail in systems for which it was not designed yet makes relatively unambiguous predictions, and for which good observations are available. We propose and perform two such tests. First, we deduce basic properties of the Ly α absorbers, making use of the technique of Schaye (2001). These can be compared directly to observations concerning the sizes and number densities of the absorbers. Second, we derive relations between the density, enclosed mass, and temperature profiles of galaxy clusters that can be directly compared to available X-ray data. Both Ly α absorbers and clusters constitute relatively simple physical systems, are well within the MOND regime, and (in the absence of dark matter) are dominated by gas that can be accurately observed, making them ideal testing grounds for MOND.

¹ Chandra Fellow.

2. MOND AND THE Ly α FOREST

As argued by Schaye (2001; hereafter S01), basic properties of the gas responsible for Ly α absorption in quasar spectra can be deduced using simple physical arguments. Along any sight line passing through a gas “cloud,” the size of the region dominating the absorption will typically be of order the local Jeans length, regardless of the overall shape of the cloud and regardless of whether the cloud as a whole is in dynamical equilibrium. Using this reasoning, S01 calculates properties of the Ly α absorbers that are in good agreement with numerical simulations and available observations. Because the absorbers are dynamically simple and have very low characteristic accelerations, MOND makes strong predictions about their properties, which we will now derive in parallel to the treatment by S01.

MOND can be formulated in a number of ways, as a modification of either inertia (e.g., Milgrom 1999a, 1999b) or gravity (e.g., Bekenstein & Milgrom 1984). In its most general incarnation, the gravitational acceleration in an “isolated” (meaning not embedded in a gravitational field with larger characteristic acceleration) system is given by

$$a = \sqrt{a_N a_0} \quad (1)$$

when $a_N \ll a_0$, where a_N is the acceleration calculated using Newtonian gravity and $a_0 \approx 1.2 \times 10^{-8} \text{ cm s}^{-2}$ (McGaugh & de Blok 1998) is the MOND acceleration parameter. (Systems that are embedded in a large external field are discussed below). This acceleration law yields a dynamical time

$$t_{\text{dyn}} \equiv \left(\frac{L}{a}\right)^{1/2} = \left(\frac{L}{\rho a_0 G}\right)^{1/4} = \left[\frac{L(1-Y)}{n_H m_p a_0 G}\right]^{1/4}, \quad (2)$$

where L and ρ are the characteristic size and density of the system, respectively, n_H is the hydrogen number density in a medium of hydrogen mass fraction $(1-Y)$, and m_p is the proton mass. The system’s sound crossing time is unchanged by MOND and is

$$t_{\text{sc}} \equiv \frac{L}{c_s} = L \left(\frac{\mu m_p}{\gamma k T}\right)^{1/2}, \quad (3)$$

where T is the temperature, $\gamma = 5/3$ is the assumed adiabatic index, and $\mu \approx 0.59$ is the mean molecular weight per particle for a fully ionized primordial plasma with $Y = 0.24$. Setting these timescales equal to each other yields the Jeans length

$$L_J = \left(\frac{1-Y}{n_H a_0 G}\right)^{1/3} \left(\frac{\gamma k T}{\mu}\right)^{2/3} m_p^{-1}. \quad (4)$$

This can be converted to a column density $N_{\text{HI}}^J = L_J n_H \times (n_{\text{HI}}/n_H)$ using the ionization correction from S01, valid for a highly ionized, optically thin plasma:

$$\frac{n_{\text{HI}}}{n_H} = n_H \frac{1-Y/2}{1-Y} \frac{\beta}{\Gamma}, \quad (5)$$

where $\beta \approx 4 \times 10^{-13} T_4^{-0.76} \text{ cm}^3 \text{ s}^{-1}$ and $\Gamma \equiv \Gamma_{12} \times 10^{-12} \text{ s}$ are the recombination and ionization rates with $T_4 \equiv T/10^4 \text{ K}$; $\Gamma_{12} \approx 1$ is measured at redshift $z \sim 3$ (see Scott et al. 2000 and references therein). The resulting Jeans column density can be expressed as a function of over-

density $\delta \equiv n_H/\bar{n}_H - 1$, as

$$\begin{aligned} N_{\text{HI}}^J &= \left(\frac{\gamma k T}{a_0^{1/2} G^{1/2} \mu m_p^4}\right)^{2/3} \left(1 - \frac{Y}{2}\right) (1-Y) \left(\frac{\beta}{\Gamma}\right) \\ &\quad \times [\rho_c^0 \Omega_b (1+\delta)]^{5/3} (1+z)^5 \\ &\approx 3.6 \times 10^{12} \text{ cm}^{-2} T_4^{-0.09} \Gamma_{12}^{-1} \left(\frac{\Omega_b h^2}{0.02}\right)^{5/3} \\ &\quad \times (1+\delta)^{5/3} \left(\frac{1+z}{4}\right)^5, \end{aligned} \quad (6)$$

where $T_4 \equiv T/10^4 \text{ K}$, ρ_c^0 is the current critical density, and Ω_b is the baryonic density parameter. Thus, isolated Ly α absorbers of density equal to the cosmic mean have about 10 times lower column density than in the cold dark matter (CDM) picture, with different dependences on T , z , etc. (cf. S01, eq. [10]). One can also express the Jeans length in terms of the observed H I column density:

$$\begin{aligned} L_J &= \left[\frac{(1-Y)(1-Y/2)}{a_0^2 G^2 m_p^6} \left(\frac{\gamma k T}{\mu}\right)^4 \left(\frac{\beta}{\Gamma}\right) N_{\text{HI}}^{-1}\right]^{1/5} \\ &\approx 11 \text{ kpc} \left(\frac{N_{\text{HI}}}{10^{14} \text{ cm}^{-2}}\right)^{-1/5} \Gamma_{12}^{-1/5} T_4^{0.65}, \end{aligned} \quad (7)$$

about a factor of 10 smaller than an absorber of the same column density in the CDM picture (S01, eq. [12]) and with different scalings for all parameters. Note that significant external pressure would only decrease this size. A few self-consistency checks are in order. First, the Newtonian acceleration is

$$a_N \approx 4 \times 10^{-13} \text{ cm s}^{-2} (N_{\text{HI}}/10^{14} \text{ cm}^{-2})^{2/5} T_4^{0.70} \Gamma_{12}^{2/5}, \quad (8)$$

verifying that the system is in the MOND regime. The internal acceleration is then $\approx a_0/170$. Second, the system’s dynamical time is

$$t_{\text{dyn}} = 2 \times 10^{16} \text{ s} (N_{\text{HI}}/10^{14} \text{ cm}^{-2})^{-1/5} T_4^{0.15} \Gamma_{12}^{-1/5}, \quad (9)$$

whereas the Hubble time² is $\approx (1.1-2.7) h_{65}^{-1} \times 10^{17} \text{ s}$ for $3 \gtrsim z \gtrsim 1$, so the absorbers are self-consistently in local hydrostatic equilibrium (assuming they can reach this equilibrium; see below).

The method of S01 can also be used to “invert” the observed column density distribution into an estimate of the total mass density in Ly α absorbers, using

$$\begin{aligned} \Omega_{\text{gas}} &= \frac{8\pi G H(z)}{3H_0^2 c(1+z)^2} \left[\frac{\gamma k T m_p \Gamma}{\mu(1-Y)(1-Y/2)\beta}\right]^{2/5} \\ &\quad \times (a_0 G)^{-1/5} \int dN_{\text{HI}} N_{\text{HI}}^{2/5} \frac{d^2 n(N_{\text{HI}}, z)}{dN_{\text{HI}} dz}, \end{aligned} \quad (10)$$

where $d^2 n(N_{\text{HI}}, z)/dN_{\text{HI}} dz$ is the differential number of observed lines of column density N_{HI} at redshift z .

The preceding calculation applies to an isolated absorber, but, because the strong equivalence principle is violated in MOND, the internal dynamics of systems can change if

² We assume that whatever cosmology MOND engenders will be a Friedmann model with a scale factor that evolves roughly as in a standard cosmology with $\Omega_m = 1 - \Omega_\Lambda = 0.3$ (as indicated by observations).

they are embedded in an external acceleration field g_0 , even if it is homogeneous (i.e., $g_0 = g_0 \hat{z}$ with coordinates such that \hat{z} is the external field direction). Milgrom (1986) shows that, in the Lagrangian formulation of MOND (Bekenstein & Milgrom 1984), if g_0 is small compared with a_0 but large compared with the internal accelerations of a system, then gravity in the subsystem is Newtonian in the coordinate system $\{x', y', z'\} \equiv \{x, y, z/2\}$ with an effective Newton's constant $G' = (a_0/g_0)G$. In this case, properties of the absorbers in MOND can be computed directly from the corresponding Newtonian/CDM expressions from S01, with those substitutions.³ For example, the size of the absorbing region is then

$$L_J \approx 40 \text{ kpc} \left(\frac{N_{\text{H I}}}{10^{14} \text{ cm}^{-2}} \right)^{-1/3} \left(\frac{a_0/g_0}{25} \right)^{-2/3} \Gamma_{12}^{-1/3} T_4^{0.41} \quad (11)$$

in the direction perpendicular to the external field and somewhat (about 2 times) longer in the parallel direction. The density parameter in Ly α absorption systems is given by the CDM calculation of S01, adjusted by a factor of $(a_0/g_0)^{-1/3} f_g^{-1/3}$, where $f_g \approx 0.16$ is the gas-to-matter mass ratio in the CDM calculation.

The above analysis gives two quite testable predictions concerning the Ly α forest in MOND. First, the total density of gas can be computed using equation (10) (for the isolated case) or equation (16) of S01 (for the external field case). Since Ly α systems are very deep in the MOND regime, there is no a priori reason to expect that this density will be at all reasonable (i.e., as compared to the nucleosynthesis value of Ω_b), and this can be assessed. Second, the characteristic sizes of absorbers, given by equations (7) and (11), can be compared to observations of lensed quasars and quasar pairs that constrain the transverse sizes of absorbers. In making both comparisons, the external field case requires a value for the mean acceleration field of Ly α absorbers at $z = 3$. This is currently not calculable but may be crudely estimated. At $z = 0$, typical mean observed accelerations can be obtained by dividing typical bulk flow velocities of $\sim 600 \text{ km s}^{-1}$ (see, e.g., Dekel et al. 1999; Dale et al. 1999) by a Hubble time, yielding $g_0/a_0 \approx 10^{-2}$; we shall take an upper limit of $g_0/a_0 \lesssim 1/50$. If the fluctuations in the Newtonian gravitational potential (which in linear theory are constant in time in an Einstein–de Sitter cosmology) do not shrink, then $g_0(z)/a_0 \lesssim 10^{-2}(1+z)^{1/2}$. This is an upper limit, and the accelerations could be significantly smaller at $z = 3$ in a MOND universe if the potential fluctuations have grown considerably since then. From equation (8) above, we see that an external field $g_0 \gtrsim a_0/170$ is required to modify the absorber internal dynamics. Thus, we can consistently consider external fields with $25 \lesssim a_0/g_0 \lesssim 170$.

We have computed the total gas density in Ly α absorbers in both the isolated and nonisolated cases using the data of Hu et al. (1995) and Petitjean et al. (1993). In the isolated case, we find $\Omega_{\text{gas}} \approx 0.008\text{--}0.009$. This is somewhat smaller than the $\Omega_{\text{gas}} \approx 0.045$ inferred from the same data in the CDM picture or using nucleosynthesis but is still

plausible—even if we assume that most baryons must be in gas in the intergalactic medium (IGM)—considering the uncertainty inherent in the analysis and the neglect of underdense and collisionally ionized hot gas. In the case of a significant external field, we find

$$\Omega_{\text{gas}} \approx 0.028 \left(\frac{a_0/g_0}{25} \right)^{-1/3} T_4^{0.59} \Gamma_{12}^{1/3} h_{65}^{-2}, \quad (12)$$

giving $0.005 \lesssim \Omega_{\text{gas}} \lesssim 0.03$; the higher end is in comfortable agreement with observational constraints.

For isolated absorbers, MOND also predicts that the low column density ($\sim 10^{14} \text{ cm}^{-2}$) absorbers have a rather small characteristic size: $\sim 10 \text{ kpc}$ versus $\sim 100 \text{ kpc}$ for Newtonian gravity with CDM. We have argued that, in a plausible external field, the absorbers should have sizes of 20–80 kpc in their long direction and one-half this in their short direction. Spectra of lensed quasars and close quasar pairs can be used to constrain the characteristic transverse sizes of Ly α absorbers. On very small (few kiloparsec) scales, absorbers are virtually identical in both sight lines (Smette et al. 1992; Dolan et al. 2000). On intermediate (tens of kiloparsecs) scales, spectra are very similar but are currently too low resolution to conclusively constrain the absorber properties across the sight lines (e.g., Bechtold et al. 1994; Smette et al. 1995). On the largest scales, statistical analyses of the probability of detecting an absorber in both sight lines lead to estimates of absorber “sizes” of several hundred kiloparsecs (e.g., Dinshaw et al. 1995; Smette et al. 1995; Crofts & Fang 1998; D’Odorico et al. 1998). These observations are slightly at odds with the MOND predictions unless g_0 is near its upper limit, but some additional considerations must be kept in mind:

1. Except on very small scales, the observations do not currently rigorously distinguish between correlated absorbers and a single absorber spanning two sight lines. Thus, we cannot directly compare the observationally deduced sizes (several hundred kiloparsecs) to the Jeans length of absorbers of the observed column density (eqs. [7] and [11]).

2. Strictly speaking, the relations given in equations (7) and (11) connect observed column density to radial dimension, whereas the observations probe the transverse extent (or correlation). However, for an “isolated” absorbing region, these dimensions are unlikely to be very different because absorbers should vary transversely on a scale comparable to the local Jeans length, which is in turn comparable to the radial extent over which the absorption occurs. In the case of a strong external field, the absorbers should be elongated in the field direction by a factor of 2.

3. The properties of absorbers derived here assume that the absorbers are not far from local dynamical equilibrium, which would *not* be true for underdense and/or very large ($\gg 100 \text{ kpc}$) absorbers with dynamical times exceeding the Hubble time. For isolated absorbers, it can be shown that regions of this size could not give rise to sufficient absorption unless their dynamical time is shorter than the Hubble time. To see this, note that requiring $t_{\text{dyn}} > t_H$ for a fixed L gives an upper limit on density via equation (2), and this in turn gives an upper limit to column density of

$$N_{\text{H I}} < 4.4 \times 10^{11} \text{ cm}^{-2} L_{100}^3 \left(\frac{t_H}{10^{17} \text{ s}} \right)^{-8} \frac{T_4^{-0.76}}{\Gamma_{12}},$$

³ This sort of behavior is not unique to the Lagrangian formulation; a similar result can be derived from the simple formulation of MOND given by eq. (1).

where $L_{100} = L/100$ kpc. This means that isolated ~ 100 kpc absorbers of column density $\sim 10^{14} \text{ cm}^{-2}$ cannot consistently be far from local dynamical equilibrium. Absorbers in an external potential g_0 can be out of equilibrium if their column density obeys

$$N_{\text{HI}} < 10^{14} \text{ cm}^{-2} L_{100} \left(\frac{t_{\text{H}}}{10^{17} \text{ s}} \right)^{-4} \left(\frac{a_0/g_0}{25} \right)^{-2} \frac{T_4^{-0.76}}{\Gamma_{12}}.$$

Thus, absorbers in a strong external field may be only marginally in equilibrium.

In summary, we find that, if the dynamics of Ly α absorbers in MOND are dominated by their self-gravity, then they are significantly smaller than observations indicate. If, however, the clouds are immersed in a (constant) acceleration field of magnitude g_0 , then their sizes can be substantially larger, and the basic properties of Ly α absorbers approach those predicted by standard gravity (with CDM) as $g_0 \rightarrow (\Omega_{\text{gas}}/\Omega_{\text{dm}})a_0 \approx 0.16a_0$, where Ω_{gas} and Ω_{dm} are the density parameters in absorbing gas and dark matter in the CDM model. The importance of external fields in low-acceleration systems is both a methodological barrier and a saving grace of MOND. The accurate description of such systems requires a (necessarily *ab initio*) calculation of the large-scale density field surrounding them, which is in turn impossible to perform rigorously without a cosmological formulation of MOND that treats its conceptual problems (in particular the issue of which accelerations, and with respect to what, should be “counted”). On the other hand, external fields can ensure that in the limit of extremely low accelerations the properties of isolated systems in MOND will not deviate wildly from their Newtonian counterparts.

3. MOND AND CLUSTERS

Like Ly α systems, clusters of galaxies are gas dominated (in the absence of dark matter) and well observed (this time via X-ray measurements), should be in local hydrostatic equilibrium, and are in the MOND acceleration regime. They also have internal accelerations larger than expected ambient acceleration fields (and comparable to those near galaxies). Thus, strong predictions regarding their structure in MOND can be made using relatively simple arguments, as follows.

For a gaseous system of mass M in hydrostatic equilibrium, M is close to the Jeans mass M_J . For pure gas with MONDian gravity,

$$M_J \equiv \rho L_J^3 = \frac{1}{a_0 G} \left(\frac{\gamma k T}{\mu m_p} \right)^2 \approx 4.6 \times 10^{12} M_\odot \left(\frac{kT}{\text{keV}} \right)^2, \quad (13)$$

using equation (4). For comparison, the observed mass-temperature relation of clusters found by Mohr, Mathiesen, & Evrard (1999) is

$$M_{\text{ICM}}^{500} \approx 4.3 \times 10^{12} M_\odot \left(\frac{kT}{\text{keV}} \right)^{1.98}, \quad (14)$$

where M_{ICM}^{500} is the enclosed mass of the X-ray gas at the radius within which its density is approximately 500 times

the cosmic mean. While only an order-of-magnitude estimate, equation (13) would at first seem to be a remarkable success of MOND, since the CDM picture has difficulty explaining the observed mass-temperature relation in detail (see, e.g., Mohr et al. 1999; Finoguenov, Reiprich, & Böhringer 2001 and references therein). The fact that MOND can roughly account (to within a factor of 2) for the mass discrepancy in clusters has been pointed out by Sanders (1999). However, a hint of trouble is suggested by the fact that equation (14) applies for a particular radius, whereas for isothermal clusters equation (13) does not. A closer look reveals that serious problems arise when the temperature profile $T(r)$ predicted by MOND for a given density profile $\rho(r)$ is compared to observations.

Consider a spherical system such as a cluster in hydrostatic equilibrium. Then the temperature and density obey

$$\frac{1}{\rho} \frac{dP}{dr} = -a, \quad (15)$$

where a is the magnitude of the radial gravitational acceleration and $P = (kT/\mu m_p)\rho$ is the pressure. For $a \ll a_0$ in MOND, this can be rewritten as

$$\frac{d \log \rho}{d \log r} + \frac{d \log T}{d \log r} = -\frac{\mu m_p}{kT} [a_0 GM(r)]^{1/2}, \quad (16)$$

where $M(r)$ is the enclosed mass. This equation immediately implies that, if $\rho(r)$ and $T(r)$ are power laws, then $T(r) \propto [M(r)]^{1/2}$, as per the Jeans argument. More generally, an increasing $M(r)$ implies that $T(r)$ increases as long as the sum of $\alpha_\rho \equiv d \log \rho / d \log r$ and $\alpha_T \equiv d \log T / d \log r$ changes more slowly than $M(r)^{1/2}$. Thus, isothermal density profiles in MOND tend to have a core that contains most of the mass (and in which the logarithmic derivatives change relatively quickly) and then fall off more quickly than r^{-3} (see Milgrom 1984). We will show that this is *not* the case for the X-ray-emitting gas that dominates the mass in observed clusters, yet clusters are observed to be nearly isothermal outside of their central regions.

This constitutes a grave challenge to MOND, which can be demonstrated using the specific cases of the Virgo, Abell 2199, and Coma Clusters, for which gas density, stellar mass, and temperature profiles are available in the literature. The analysis is shown in Figures 1, 2, and 3. The top left panel of Figure 1 shows the cluster gas density deprojected from a *ROSAT* X-ray emission profile by Nulsen & Böhringer (1995), normalized to the critical density, assuming a distance to M87 of 16 Mpc. The density can be extended to $r > 200$ kpc using the β -model fit by Schindler, Binggeli, & Böhringer (1999) at large radii. The top right panel of Figure 1 shows the integrated gas mass, as well as integrated stellar mass from Schindler et al. (1999), with a contribution for M87 with $M/L_B = 8$ included from Giraud (1999). As discussed below, the details of these assumptions matter very little. The bottom left panel of Figure 1 shows the Newtonian acceleration at r , which is below the MOND parameter for $r \gtrsim 20$ kpc; the MONDified acceleration⁴ is also plotted, along with the dynamical time $(l/a)^{1/2}$ in units of the $z = 0$ Hubble time. Given this information, equation

⁴ We use the same interpolation formula in the transition region as Milgrom (1983b) and Begeman, Broeils, & Sanders (1991), i.e., $a\mu(a/a_0) = a_N$, where $\mu(x) = x/(1 + x^2)^{1/2}$.

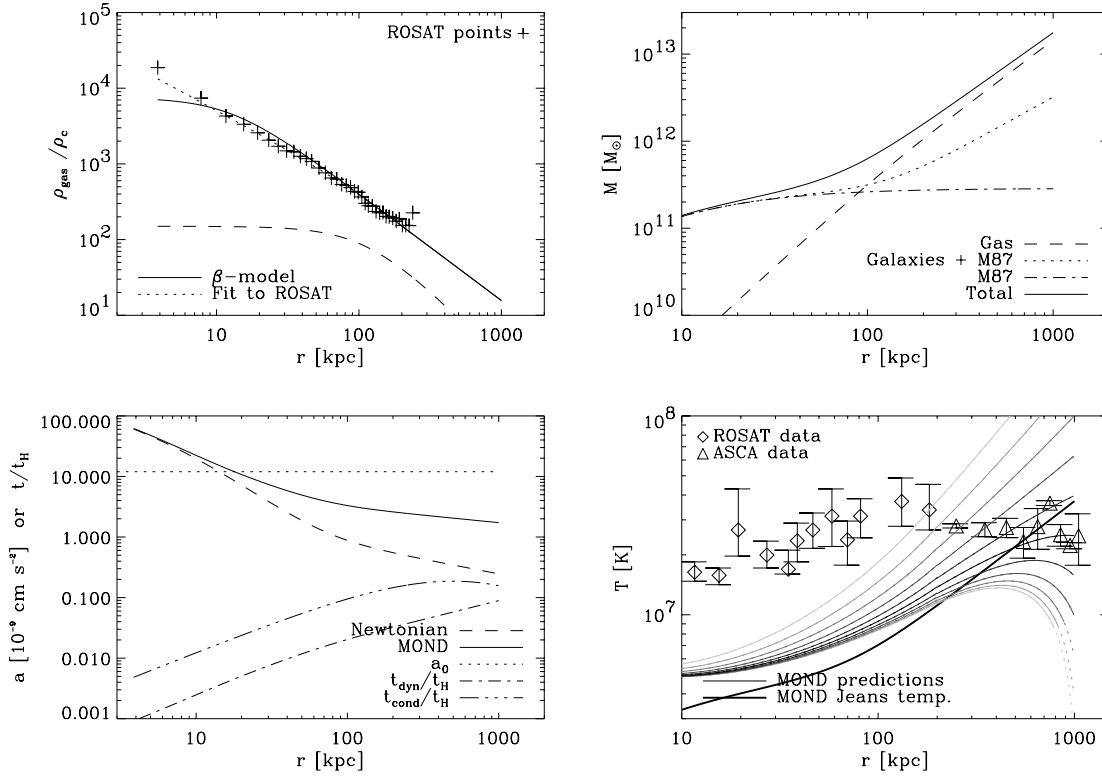


FIG. 1.—Predicted MOND temperature profile for the Virgo Cluster. *Top left*: X-ray gas density profile in units of the critical density, from Nulsen & Böhringer (1995; *plus signs*). The dotted line is a Hernquist model fit at (and used here at) $r \lesssim 200$ kpc by Giraud (1999); the solid line is a β -model, fitted by Schindler et al. (1999) at large radii (*solid line*) and used here at $r > 200$ kpc. *Top right*: Integrated mass in gas and galaxies. The mass of M87 is from Giraud (1999) with $M/L_B = 8$; we also add a component representing galaxies from Schindler et al. (1999). *Bottom left*: Newtonian and MONDian acceleration (in units of $10^{-9} \text{ cm s}^{-2}$) at each radius, showing that the cluster is deep in the MOND regime for $r \gg 20$ kpc. Also plotted are the MOND dynamical time t_{dyn} and the conduction timescale t_{cond} , both in units of the $z = 0$ Hubble time. *Bottom right*: Predicted temperature profiles, starting at 1 Mpc with temperatures between 0.1 and 10 times the (*ASCA*) observed temperature there. *ROSAT* (Nulsen & Böhringer 1995, deprojected) and *ASCA* (Shibata et al. 2001, projected) temperature profiles with 1σ error bars are shown for comparison. The heavy solid line is the MOND “Jeans temperature,” $T_J \equiv (\mu m_p/k)(a_0 GM)^{1/2}$.

(16) can be used to predict $T(r)$ given a starting $T(r_0)$. The lower right panel of Figure 1 shows this prediction, integrating inward⁵ starting at $r_0 \approx 1$ Mpc, with $T(r_0)$ taking values between 1/10 and 10 times the measured *ASCA* temperature there. If MOND were correct, one of these profiles should roughly match the observed temperatures, but none of them do. Figures 2 and 3 show the same analysis for Abell 2199 and Coma, somewhat richer and more relaxed clusters. The results are quite similar.

We have verified that the results are robust to reasonable changes in the distances to the clusters, the mean molecular weight, and the MOND interpolation formula used. We have also experimented with different profiles and normalizations for the stellar mass distribution; these do not significantly affect the results unless the stellar mass is so large ($M/L \gg 20$) as to imply the presence of dark matter (dark matter is discussed below). Significantly larger values of the MOND constant ($a_0 \gtrsim 5 \times 10^{-8} \text{ cm s}^{-2}$) help improve the fit because (as demonstrated by the agreement of eqs. [13] and [14]) the MOND “Jeans temperature” $T_J^{\text{MOND}} \equiv (\mu m_p/k)(a_0 GM)^{1/2}$ roughly agrees with observed cluster temperatures at large radii. Increasing a_0 moves this agreement to intermediate radii but still cannot yield a reasonable fit of the entire profile (and would be incompatible with the value

required by galaxy rotation curves and make Ly α absorbers even smaller).

As alluded to above, the difficulty in accounting for the cluster data in MOND—even when a_0 is allowed to vary—can be understood in more general terms using an inequality derived from equation (16) that applies to any range $[r_1, r_2]$ over which the temperature is nonincreasing:

$$\frac{\alpha_p(r_2) + \alpha_T(r_2)}{\alpha_p(r_1) + \alpha_T(r_1)} \geq \left[\frac{M(r_2)}{M(r_1)} \right]^{1/2}. \quad (17)$$

Convective stability requires that $|\alpha_T| < \frac{2}{3}|\alpha_p|$ lest entropy gradients be erased on a sound crossing time (Sarazin 1988, p. 165), giving

$$\frac{M(r_2)}{M(r_1)} \leq \left[\frac{5\alpha_p(r_2)}{3\alpha_p(r_1)} \right]^2. \quad (18)$$

In Virgo, for example, $M(r)$ increases by a factor of ≈ 25 between 100 and 1000 kpc, where the gas is observed to be roughly isothermal. However, then $\alpha_p(r = 100 \text{ kpc}) \approx -1.3$ requires (in MOND) that $\alpha_p(r = 1000 \text{ kpc}) \approx -3.9$, while $\alpha_p \approx -1.5$ is observed. Both power-law indices and total baryonic mass are very well constrained quantities, so this is a serious violation. Cluster gas density profiles are generally well fitted at large radii by β -models of form

$$\rho(r) = \rho_0 \left[1 + \left(\frac{r}{r_0} \right)^2 \right]^{3\beta/2}. \quad (19)$$

⁵ The integration can also be performed outward, matching the observed temperature at small radii, with essentially the same results.

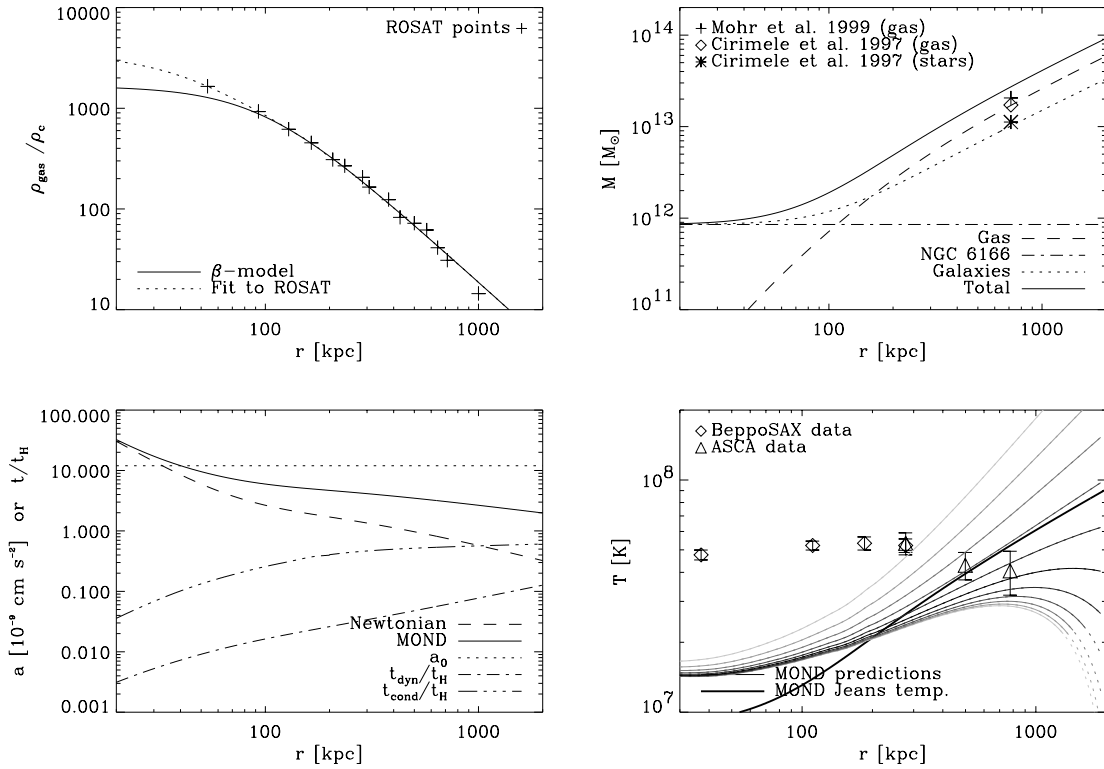


FIG. 2.—Predicted MOND temperature profile for Abell 199. *Top left*: X-ray gas density profile in units of the critical density, from Siddiqui, Stewart, & Johnstone (1998; *plus signs*; dotted line is a spline fit), with the β -profile of Markevitch et al. (1999; *solid line*) fitted at large radii and used here at $r > 200$ kpc. Adjusted to $h = 0.7$. *Top right*: Integrated mass in gas and galaxies. The central galaxy NGC 6166 is taken (conservatively) to be a point mass with $M_V = -23.47$ (Gebhardt et al. 1996) and $M/L_V = 8$; we also add a component representing galaxies proportional to the gas mass as per Cirimele, Nesci, & Trevese (1997) with amplitude chosen so as to give total mass fraction in stars at $1 h_{50}^{-1}$ Mpc equal to theirs. *Bottom left*: Newtonian and MONDian acceleration at each radius, showing that the cluster is deep in the MOND regime for $r \gg 30$ kpc. Also plotted are the MOND dynamical time t_{dyn} and the conduction timescale t_{cond} , both in units of the $z = 0$ Hubble time. *Bottom right*: Predicted *projected* temperature profiles, starting at 2 Mpc with temperatures between 0.1 and 10 times the (ASCA) observed temperature there. *BeppoSAX* (Irwin & Bregman 2000) and *ASCA* (Markevitch et al. 1999) temperature profiles with 2σ errors are shown for comparison. The heavy solid line is the MOND “Jeans temperature,” $T_J \equiv (\mu m_p/k)(a_0 GM)^{1/2}$.

In this case $\alpha(r)/\alpha(r_0) = 2/[1 + (r_0/r)^2] < 2$. Therefore, if $M(r)/M(r_0) > (10/3)^2 \approx 11$ at any radius within which the cluster has a nonrising temperature and within which the density profile is well fitted by a β -model, then MOND is violated. If $T(r)$ is exactly constant, the constraint is stronger and $M(r)/M(r_0) > 4$ violates MOND.

Since the relevant properties of Virgo, A2199, and Coma [isothermal or radially declining temperatures, increasing $M(r)$, and slowly changing $d \log \rho / d \log r$ as in the β -model] seem generic in clusters at large radii (Neumann & Arnaud 1999; Finoguenov, David, & Ponman 2000; Irwin, Bregman, & Evrard 1999), it is very hard to see how to reconcile MOND with the observations. A few possibilities that do *not* seem able to satisfactorily effect this reconciliation are:

Clusters are not in hydrostatic equilibrium.—The $z = 0$ Hubble time greatly exceeds the dynamical time (see bottom left panels of Figs. 1, 2, and 3) and the sound crossing time, inside ~ 1 Mpc, so hydrostatic equilibrium should hold within that radius (see Sarazin 1988 for some discussion). Moreover, simulations (albeit in the CDM picture) show that hydrostatic equilibrium and spherical symmetry are good assumptions in inferring the gravitational force given observed density and temperature profiles (Schindler 1996). Finally, we note that the observed magnetic fields in clusters do not appear sufficiently strong to significantly affect the force balance or the inferred cluster

bulk properties (e.g., Gonçalves & Friaca 1999; Dolag, Evrard, & Bartelmann 2001).

Measured temperatures are incorrect.—While temperature determinations do have significant errors (especially in *ROSAT* data), the predicted MOND temperature profile disagrees by many σ from the *ASCA* measurements in Virgo, from *ASCA* and *BeppoSAX* measurements in A2199, and from *XMM* measurements in Coma. More generally, there is no indication in observations using *ASCA* (e.g., Markevitch et al. 1998; White 2000; Finoguenov, Arnaud, & David 2001), *BeppoSAX* (Irwin & Bregman 2000), or *XMM* (Arnaud et al. 2001a, 2001b) that clusters have steeply rising temperatures at large radii.

Efficient conduction causes clusters to be isothermal.—Figure 1 gives the conduction timescale (Sarazin 1988)

$$t_{\text{cond}} \approx \frac{5n_e r^2 k}{2\kappa(T)}, \quad (20)$$

where

$$\kappa(T) = 2 \times 10^{11} \left(\frac{kT}{\text{keV}} \right)^{5/2} \text{ ergs s}^{-1} \text{ K}^{-1}. \quad (21)$$

This is a lower limit because it neglects magnetic fields, which could increase the conduction time by a factor of

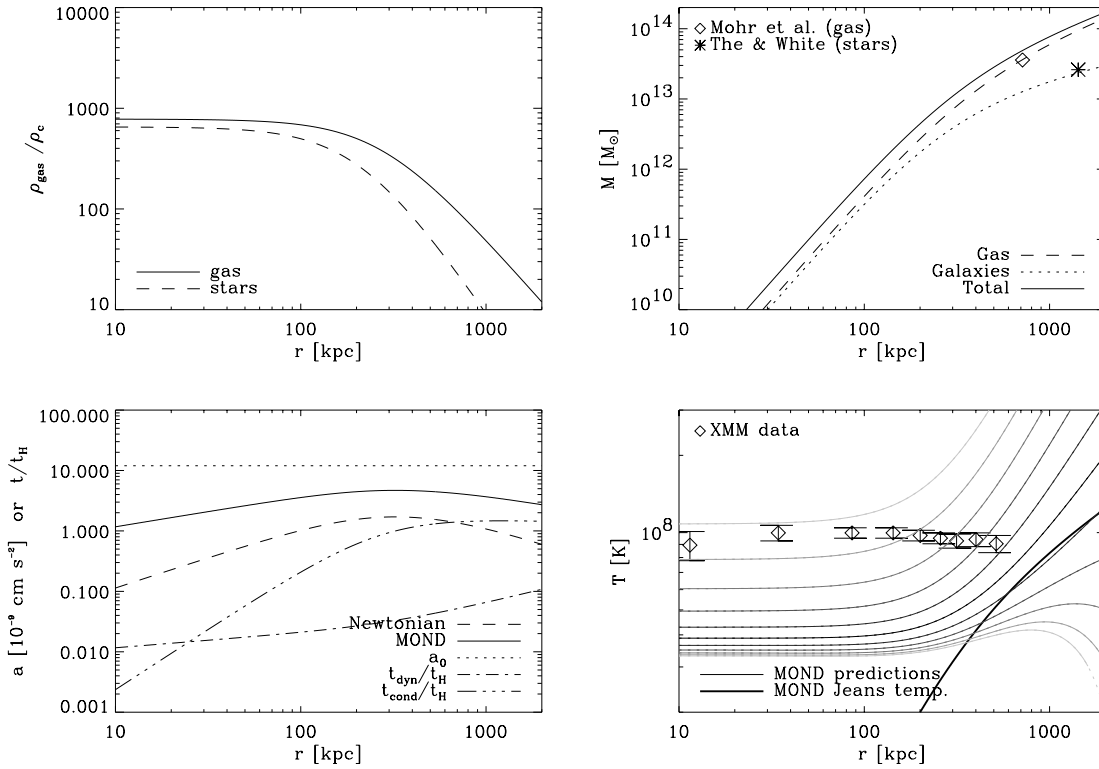


FIG. 3.—Predicted MOND temperature profile for Coma. *Top left*: X-ray gas density profile (solid line), using the β -model fit of Mohr et al. (1999), adjusted to $h = 0.7$. The dashed line is the galaxy stellar mass density, using $M/L_V = 8$ and luminosity density from The & White (1988). *Top right*: Integrated mass in gas and stars. *Bottom left*: Newtonian and MONDian acceleration at each radius, showing that the cluster is deep in the MOND regime for all radii. Also plotted are the MOND dynamical time t_{dyn} and the conduction timescale t_{cond} , both in units of the $z = 0$ Hubble time. *Bottom right*: Predicted projected temperature profiles, starting at 2 Mpc with temperatures between 0.1 and 10 times the observed temperature there. The XMM temperature profile (Arnaud et al. 2001b) with 2σ errors is shown for comparison. The heavy solid line is the MOND “Jeans temperature,” $T_J \equiv (\mu m_p/k)(a_0 GM)^{1/2}$.

between several and several thousand (see, e.g., Rosner & Tucker 1989 and Chandran & Cowley 1998, respectively). If $t_{\text{cond}} \lesssim t_{\text{Hub}}$ for some range in radius, we would expect to see a nearly isothermal temperature profile there. However (and regardless of whether or not $t_{\text{cond}} \lesssim t_{\text{dyn}}$), the cluster density profile would respond to this conduction by readjusting to restore hydrostatic equilibrium on a dynamical time. However, then (by an inverted version of the argument given above), MOND would predict a density profile with quickly varying logarithmic derivatives, contradicting the observed density profile. In other words, equation (16) prescribes a one-to-one relation between $\rho(r)$, $M(r)$, and $T(r)$, demonstrated in Figures 1 and 2. Since the predicted MOND $T(r)$ is not isothermal, an isothermal $T(r)$ cannot match the observed $\rho(r)$.

Observed density profiles are incorrect.—It has been proposed that a multiphase medium in clusters in which one component has a small filling factor could lead to an overestimate of the gas density in X-ray measurements (e.g., White & Fabian 1995; Gunn & Thomas 1996). If this effect existed and were more severe at large radii, the observationally inferred density profile could be flatter than the true profile, which could have more quickly varying α_p . However, studies of this effect find that the mass discrepancy is likely to be relatively small ($\ll 50\%$) and, moreover, less important at large radii (White & Fabian 1995; Gunn & Thomas 1996; Nagai, Sulkanen, & Evrard 2000). The comparison between masses inferred from Sunyaev-Zeldovich measurements ($\propto n_e$) and X-ray emission mea-

surements ($\propto n_e^2$) also disfavors large corrections (Grego et al. 2001; Patel et al. 2000; Nagai et al. 2000).

Based on observations of an apparent excess of extreme-UV (EUV) emission, it has also been claimed that clusters may contain a large mass of warm ($\sim 10^6$ K) gas (e.g., Lieu, Bonamente, & Mittaz 2000; Bonamente, Lieu, & Mittaz 2001). If this is the case, it would be extremely favorable to the MOND hypothesis. Note, however, that another group, while finding EUV excess, finds a significantly smaller intensity (e.g., Bowyer, Korpela, & Berghöfer 2001) and that *FUSE* observations place tight limits on warm gas in Coma and Virgo, which are inconsistent with the proposed models (Dixon et al. 2001).

There is dark matter in clusters.—One might argue that there is a strongly concentrated component of baryonic dark matter in clusters (Milgrom 1999b; Sanders 1999), leading to nearly isothermal temperatures where that component dominates the gravitational mass. Using our calculations, we can estimate the required amount of dark matter. To do so, we have fitted dark matter density profiles of various (Navarro, Frenk, & White 1997 [NFW], β -model, Hernquist model) parametric forms,⁶ while constraining the ratio ξ_1 of enclosed dark mass to enclosed gas mass at 1 Mpc. By lowering this ratio, we can find, for each parametric form, the lowest value of ξ_1 for which a plausible

⁶ We have also tried several more general forms with no significant effect on the conclusions.

fit can be found. All three models yield fairly good fits if ξ_1 is left free and yield $\xi_1 \approx 4$ –5 for Coma, $\xi_1 \approx 2$ –2.5 in A2199, and $\xi_1 \approx 1$ –2 in Virgo. When ξ_1 is fixed and progressively lowered, we find minimal allowed values of $\xi_1 \approx 3$ for Coma, $\xi_1 \approx 1.5$ for A2199, and $\xi_1 \approx 1$ for Virgo.⁷ The analogous ratios at 200 kpc take approximate minimal values of 11, 13, and 7.5, respectively. The details of the fits depend on h , a_0 , the MOND interpolation formula, and (of course) the parametric form chosen, but the general result that MOND requires dark matter of at least 1 and up to several times the gas mass within 1 Mpc, and about 10 times the gas mass within 200 kpc, is robust unless $h < 0.5$ or $a_0 > 2 \times 10^{-8} \text{ cm s}^{-2}$.

The issues we have addressed in this section have been considered before by Gerbal et al. (1992, 1993), who computed $M(r)$ using observed (but extrapolated) $\rho(r)$ and the assumption of isothermality. This yielded $M(r)$ somewhat larger than the observed mass. Milgrom (1993) criticized this approach and suggested a different one similar to that employed here. Using the Coma Cluster, The & White (1988) tested whether they could generate a set of $\rho(r)$, $M(r)$, and $T(r)$ in MOND that could match the observations available at that time. They succeeded, but only by using $h = 0.5$ and $a_0 = 2 \times 10^{-8} \text{ cm s}^{-2}$ (which are not now observationally viable). We have reproduced their calculations but find that, even with their parameters, the now-available accurate temperature profile of Coma cannot be fitted.

Thus, it seems that while MOND can account for the non-Keplerian form of galactic rotation curves (and, somewhat surprisingly, for the mass-temperature relation in clusters), it cannot account for cluster density and temperature profiles in detail. The difference in success derives from the fact that, roughly speaking, in MOND an asymptotically isothermal temperature profile corresponds to a point mass, whereas clusters are extended yet still in the MOND acceleration regime. In CDM cosmology the isothermality of both galaxies and clusters is explained by assuming that both are embedded in an isothermal dark halo that dominates the mass.

4. DISCUSSION AND CONCLUSIONS

MOND as an alternative to the dark matter hypothesis has generally fared quite well when applied to galaxies. However, galaxies can test MOND only in the limited regime of accelerations of $(0.1\text{--}1)a_0$ and physical scales of less than 100 kpc. It is therefore important to discover whether MOND's success extends to systems at much lower accelerations and/or much greater physical scales. To this end, we have predicted various properties of Ly α absorbers and galaxy clusters in MOND, using hydrostatic equilibrium arguments. Both types of systems are observationally well constrained, and well within the MOND acceleration regime.

We find that, as compared to their properties in the CDM picture, the Ly α absorbers in MOND have some-

what higher characteristic density and smaller characteristic size for a given column density, potentially in conflict with absorption studies of quasar pairs and lenses. The magnitude of the effect, however, depends on the (unknown) magnitude of the external acceleration field in which they are embedded, since MOND violates the strong equivalence principle,⁸ and, if the ambient acceleration field is large, then the predicted absorber properties can approach those observed. When combined with the observed differential number density of absorption lines, the analysis yields (for any assumed external field) a reasonable density of intergalactic gas (as does the CDM picture). A more accurate prediction of the detailed physical and statistical properties of Ly α absorbers in MOND—which match observations in detail in the CDM case—will probably require a (presently infeasible) ab initio calculation of the large-scale acceleration field and the absorbers themselves.

We note also that the MOND Jeans mass depends only on temperature:

$$M_J \approx 3.4 \times 10^6 T_4^2 M_\odot, \quad (22)$$

and gives a rather small Jeans mass in the IGM, which may dramatically alter galaxy formation in MOND (although we have not pursued that issue here).

Simple arguments can also predict the mass-temperature relation in clusters, and the temperature profile of any single cluster given its observed gas density and enclosed mass profile. The MOND-predicted M - T relation is impressively close to the observed one, although this success seems coincidental, because it is sensitive to the radius at which the enclosed mass is measured (since in MOND the Jeans mass depends only on the temperature and the clusters are roughly isothermal).

Stronger constraints can be derived using the observed mass, temperature, and density profiles of clusters: given hydrostatic equilibrium, MOND directly predicts the relation between the three quantities. For the form of mass and gas density profiles generally observed, MOND predicts rising temperature profiles. In the specific cases of the Virgo, Abell 2199, and Coma Clusters, we have shown that MOND's predictions strongly disagree with measurements from *ASCA*, *ROSAT*, *BeppoSAX*, and *XMM*, and we see no reasonable way to effect a reconciliation without recourse to large amounts of (presumably baryonic) dark matter of an unknown type. For these clusters, the mass of such dark matter must exceed the gas mass within 1 Mpc by a factor of ~ 1 –3, and by a factor of about 10 within 100 kpc. Moreover, we have argued that the discrepancy applies to clusters in general. This may be interpreted as a failure of MOND to describe cluster dynamics in terms of their observed baryonic content or as a bold prediction (Sanders 1999) that we have so far observed only a minority of their baryonic content. (Discovery of such dark matter would also constitute a serious crisis for the CDM model.)

In conclusion, we find that, although MOND can explain the rotation curves of galaxies in a simple and compelling way, it is less effective in extended systems such as clusters and (perhaps) intergalactic gas clouds, in which the visible mass cannot be described as a gravitational point mass

⁷ Note that we are able to fit temperature profiles—in standard gravity—using NFW profiles with $7 \lesssim \xi_1 \lesssim 9$ and concentration parameters between ~ 3 and 4 (for Coma) and ~ 7 and 10 (A2199 and Virgo). The concentration for Coma is perhaps somewhat low, but the results seem otherwise reasonable.

⁸ This effect, incidentally, severely limits the possibility of testing the MOND formula over many decades of acceleration.

when the system is in the MOND regime. This implies that dark matter (or perhaps some different modification of gravity) is required to accurately describe such systems.

We thank Simon White, Stacy McGaugh, Moti Milgrom, David Spergel, Ned Wright, and Neta Bahcall for helpful

suggestions. This work was supported by a grant from the W. M. Keck foundation. E. Q. is supported by NASA through *Chandra* Fellowship PF9-10008, awarded by the *Chandra* X-Ray Center, which is operated by the Smithsonian Astrophysical Observatory for NASA under contract NAS 8-39073.

REFERENCES

- Arnaud, M., Neumann, D. M., Aghanim, N., Gastaud, R., Majerowicz, S., & Hughes, J. P. 2001a, *A&A*, 365, L80
 Arnaud, M., et al. 2001b, *A&A*, 365, L67
 Bechtold, J., Crotts, A. P. S., Duncan, R. C., & Fang, Y. 1994, *ApJ*, 437, L83
 Begeman, K. G., Broeils, A. H., & Sanders, R. H. 1991, *MNRAS*, 249, 523
 Bekenstein, J., & Milgrom, M. 1984, *ApJ*, 286, 7
 Bonamente, M., Lieu, R., & Mittaz, J. P. D. 2001, *ApJ*, 546, 805
 Bowyer, S., Korpela, E., & Berghöfer, T. 2001, *ApJ*, 548, L135
 Chandran, B., & Cowley, S. 1998, *Phys. Rev. Lett.*, 80, 3077
 Cirimele, G., Nesci, R., & Trevese, D. 1997, *ApJ*, 475, 11
 Crotts, A. P. S., & Fang, Y. 1998, *ApJ*, 502, 16
 Dale, D. A., Giovanelli, R., Haynes, M. P., Campusano, L. E., Hardy, E., & Borgani, S. 1999, *ApJ*, 510, L11
 de Blok, W. J. G., & McGaugh, S. S. 1998, *ApJ*, 508, 132
 Dekel, A., Eldar, A., Kolatt, T., Yahil, A., Willick, J. A., Faber, S. M., Courteau, S., & Burstein, D. 1999, *ApJ*, 522, 1
 Dinshaw, N., Foltz, C. B., Impey, C. D., Weymann, R. J., & Morris, S. L. 1995, *Nature*, 373, 223
 Dixon, W. V. D., Sallmen, S., Hurwitz, M., & Lieu, R. 2001, *ApJ*, 550, L25
 D'Odorico, V., Cristiani, S., D'Odorico, S., Fontana, A., Giallongo, E., & Shaver, P. 1998, *A&A*, 339, 678
 Dolag, K., Evrard, A., & Bartelmann, M. 2001, *A&A*, 369, 36
 Dolan, J. F., Michalitsianos, A. G., Nguyen, Q. T., & Hill, R. J. 2000, *ApJ*, 539, 111
 Finoguenov, A., Arnaud, M., & David, L. P. 2001, *ApJ*, 555, 191
 Finoguenov, A., David, L. P., & Ponman, T. J. 2000, *ApJ*, 544, 188
 Finoguenov, A., Reiprich, T. H., & Böhringer, H. 2001, *A&A*, 368, 749
 Gebhardt, K., et al. 1996, *AJ*, 112, 105
 Gerbal, D., Durret, F., Lachize-Rey, M., & Lima-Neto, G. 1992, *A&A*, 262, 395
 ———, 1993, *A&A*, 273, L9
 Giraud, E. 1999, *ApJ*, 524, L15
 Gonçalves, D. R., & Friaca, A. C. S. 1999, *MNRAS*, 309, 651
 Grego, L., Carlstrom, J., Reese, E., Holder, G., Holzapfel, W., Marshall, J., Mohr, J., & Patel, S. 2001, *ApJ*, 552, 2
 Gunn, K. F., & Thomas, P. A. 1996, *MNRAS*, 281, 1133
 Hu, E. M., Kim, T., Cowie, L. L., Songaila, A., & Rauch, M. 1995, *AJ*, 110, 1526
 Irwin, J. A., & Bregman, J. N. 2000, *ApJ*, 538, 543
 Irwin, J. A., Bregman, J. N., & Evrard, A. E. 1999, *ApJ*, 519, 518
 Lieu, R., Bonamente, M., & Mittaz, J. P. D. 2000, *A&A*, 364, 497
 Markevitch, M., Forman, W. R., Sarazin, C. L., & Vikhlinin, A. 1998, *ApJ*, 503, 77
 Markevitch, M., Vikhlinin, A., Forman, W. R., & Sarazin, C. L. 1999, *ApJ*, 527, 545
 McGaugh, S. S., & de Blok, W. J. G. 1998, *ApJ*, 499, 66
 Milgrom, M. 1983a, *ApJ*, 270, 365
 ———, 1983b, *ApJ*, 270, 371
 ———, 1983c, *ApJ*, 270, 384
 ———, 1984, *ApJ*, 287, 571
 ———, 1986, *ApJ*, 302, 617
 ———, 1993, *A&A*, 273, L5
 ———, 1999a, preprint (astro-ph/9805346)
 ———, 1999b, in *Dark Matter in Astrophysics and Particle Physics*, ed. H. V. Klapdor-Kleingrothaus & L. Baudis (Bristol: IOP), 443
 Mohr, J. J., Mathiesen, B., & Evrard, A. E. 1999, *ApJ*, 517, 627
 Nagai, D., Sulkanen, M. E., & Evrard, A. E. 2000, *MNRAS*, 316, 120
 Navarro, J., Frenk, C., & White, S. D. M. 1997, *ApJ*, 490, 493
 Neumann, D. M., & Arnaud, M. 1999, *A&A*, 348, 711
 Nulsen, P. E. J., & Böhringer, H. 1995, *MNRAS*, 274, 1093
 Patel, S. K., et al. 2000, *ApJ*, 541, 37
 Peebles, P. J. E. 1999, *PASP*, 111, 274
 Petitjean, P., Webb, J. K., Rauch, M., Carswell, R. F., & Lanzetta, K. 1993, *MNRAS*, 262, 499
 Rosner, R., & Tucker, W. H. 1989, *ApJ*, 338, 761
 Sanders, R. H. 1996, *ApJ*, 473, 117
 ———, 1999, *ApJ*, 512, L23
 ———, 2000, *MNRAS*, 313, 767
 Sanders, R. H., & Verheijen, M. A. W. 1998, *ApJ*, 503, 97
 Sarazin, C. 1988, *X-Ray Emission from Clusters of Galaxies* (Cambridge: Cambridge Univ. Press)
 Schaye, J. 2001, *ApJ*, 559, 507
 Schindler, S. 1996, *A&A*, 305, 756
 Schindler, S., Binggeli, B., & Böhringer, H. 1999, *A&A*, 343, 420
 Scott, J., Bechtold, J., Dobrzycki, A., & Kulkarni, V. P. 2000, *ApJS*, 130, 67
 Shibata, R., Matsushita, K., Yamasaki, N. Y., Ohashi, T., Ishida, M., Kikuchi, K., Böhringer, H., & Matsumoto, H. 2001, *ApJ*, 549, 228
 Siddiqui, H., Stewart, G. C., & Johnstone, R. M. 1998, *A&A*, 334, 71
 Smette, A., Robertson, J. G., Shaver, P. A., Reimers, D., Wisotzki, L., & Koehler, T. 1995, *A&AS*, 113, 199
 Smette, A., Surdej, J., Shaver, P. A., Foltz, C. B., Chaffee, F. H., Weymann, R. J., Williams, R. E., & Magain, P. 1992, *ApJ*, 389, 39
 The, L. S., & White, S. D. M. 1988, *AJ*, 95, 1642
 Turner, M. S. 1999, *PASP*, 111, 264
 van den Bosch, F. C., & Dalcanton, J. J. 2000, *ApJ*, 534, 146
 White, D. A. 2000, *MNRAS*, 312, 663
 White, D. A., & Fabian, A. C. 1995, *MNRAS*, 273, 72